9th Asia-Pacific Conference on Wind Engineering
Auckland, New Zealand
3-7 December 2017

An Acrosswind Equivalent Static Wind Load Model for Rectangular Shaped Tall Buildings

C.M. Cheng, J. Wang and T.C. Lai

Wind Engineering Research Center
Tamkang University, New Taipei City, Taiwan

Abstract

In this article, an acrosswind equivalent static wind load model for rectangular shaped tall buildings were proposed based on wind tunnel data. In the proposed acrosswind force spectral model, specific physical meanings are given to the key parameters. In such a way, the empirical model is more in line with current understanding on building acrosswind loads, it can be improved by others with support of additional data. The lift coefficients and spectral estimates produced by the proposed model were compared with wind tunnel measurements with satisfactory results. A large number of prototype tall buildings were used to study the model performance in term of building overturning moment. For most cases, the base moment yielded by proposed ESWL model are either within 10% error bound or slightly conservative.

Introduction

In typhoon-prone regions such as Taiwan, wind load is an important factor for building design. It is well known that buildings are subjected to alongwind, acrosswind and torsional wind loads. For majority of the low-rise buildings, the alongwind load induced by approaching atmospheric turbulent boundary layer flow is the dominant wind load. The fundamental frame work for alongwind load was laid in 1960s by A.G. Davenport. The alongwind ESWL for building is now well-established and has been adopted by many wind codes in various forms. However, for many tall or super tall builidngs, acrosswind load bears equal or more weight than alongwind load in wind resistant design. The acrosswind load is primarily caused by vortex shedding phenomenon, which is sensitive to building shape and turbulence Therefore, for the commonly seen rectangular shaped tall buildings, there exists no valid theoretical or semi-analytical model to describe the acrosswind load. Current practices in various wind codes can be categorized into three types, they are: (i) acknowledge the importance of vortex induced acrosswind load and designate the response to building designer, such as ASCE7-16 (2016); (ii) adopting empirical formulae derived from wind tunnel data, such as AIJ recommendations (2004) or Australian/New Zealand Standard (2002). Empirical acrosswind load model, such as the one in AIJ-2004, AS/NZS1170.2:2011 or the mathematical formulae proposed by Liang et al., (2004), Tang et al (2010), parameters such as side ratio, aspect ratio, flow features are all or partially included. In those empirical formulae, in order to simulate the general shape of acrosswind force spectra, fractional mathematical expression were chosen to be the basic spectral form without clear physical meaning. Combining with proper lift force coefficient, these empirical models can produce reasonable acrosswind loads. However, these empirical models are difficult to adjust or improve, especially by a second party, due to lacking of physical meanings. This paper intends to build an empirical acrosswind equivalent static wind load model that holds sufficient physical meaning and can be further modified with additional experimental data even by others.

Aerodynamic data

All wind tunnel tests were conducted in an open-circuit, suction type wind tunnel with test section of 17m in length, 2m in width and 1.5m in height. Three turbulent boundary layer flows, designated by BL-A, BL-B, BL-C, with power law index α=0.32, 0.25, 0.15, were generated to represent wind profiles over urban, suburban and open country terrains, respectively.

Acrylic pressure models and high speed electronic pressure scanner system were used in wind tunnel experiment. The geometry variations of the pressure models are: 11 sets of aspect ratio: $H/\sqrt{BL}$ =2, 2.5, 3, 3.5, 4, 4.5, 5, 5.5, 6, 6.5, 7; 13 sets of side ratios: L/B= 1/5, 1/4, 1/3, 1/2.5, 1/2, 1/1.5 1/1, 1.5/1, 2/1, 2.5/1, 3/1, 4/1, 5/1. All models have same cross-sectional area, (BL)=100cm^2 i.e., same model height for a particular aspect ratio, $H/\sqrt{BL}$. The sampling rate was 200Hz and the sample length was 287 seconds. During model testing, Blockage ratio is less than 5%. Reynolds number for the upper half of the testing model was kept greater than 4×10^4 which is higher than $R_{e,cr}\approx2\times10^4$ required for Reynolds number similarity.

Shown in Figure 1 are the RMS base lift coefficients, C_L (defined in Eq.(2)), of building in three different flow fields. Since all models have same cross-sectional area and C_L was normalized with respect to breadth, B. C_L is primarily reflecting the side face area on which the acrosswind load asserted. Flow field condition and aspect ratio cast secondary effects. In urban terrain flow filed, *BL-A*, C_L decreases with aspect ratio for all side ratio cases and increases with side ratio for all aspect ratio cases. In *BL-B* and *BL-C*, C_L increases with increase of side ratio in general; however, for *L/B*=1.0~3.0, C_L decreases with increase of side ratio due to reattachment phenomenon. For the model with smaller side ratio, lateral faces are subjected to bigger suctions due to complete vortex shedding, but the base lift force is reduced due to the relatively shorter side faces.

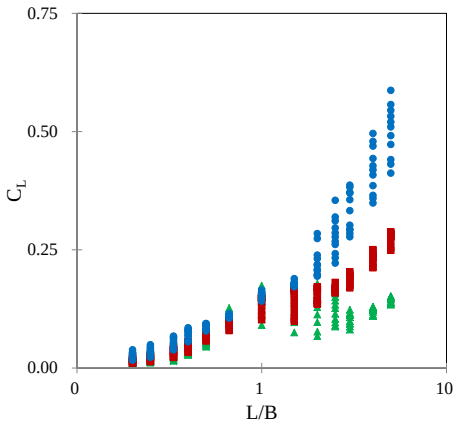

Figure 1. Variation of RMS base lift force coefficients. ●：BL-A，■：BL-B，▲：BL-C

The effect of side ratio, *L/B*, on reduced generalized acrosswind force spectra in suburban flow field, *BL-B*, is shown in Figure 2. The spectra of various side ratio can be categorized into two groups. For models with side ratio less than 1.0, the lift spectra show significantly high energy contents near the Strouhal frequency of $fB/U_H \approx 0.1$. For $L/B>1$, spectral peak induced by vortex shedding gradually reducing and move towards lower frequency as reattachment becomes more obvious and consequently narrowing the separation wake. At the same time, a second spectral peak induced by reattachment and rear end separation gradually emerges especially for large aspect ratio and in open terrain flow field, *BL-C*. For buildings with low aspect ratio, end effects and high turbulence intensity tend to obscure spectral peaks induced by vortex shedding and reattachment. It also can be observed that higher turbulence intensity will increase the spectral bandwidth, thus, increase the spectral estimates in higher frequency region where buildings natural frequencies are. It is also noticed that for models with low aspect ratio, $H/\sqrt{BL} = 2$ & 2.5, the trend of spectral energy cascade slow down rapidly as if there exist a new energy source in higher frequency region. It can only be attributed to the three dimensional effects from the free end at building top and fixed end at bottom. This 3-dimensional effect makes buildings acrosswind force spectra more complex and unpredictable. It will become an obstacle to be overcome in constructing an empirical model for it.

Figure 2. Reduced spectra of generalized acrosswind force of buildings with aspect ratio, H/√BL=6, in BL-B. —：L/B=0.2，—：L/B=0.33，—：

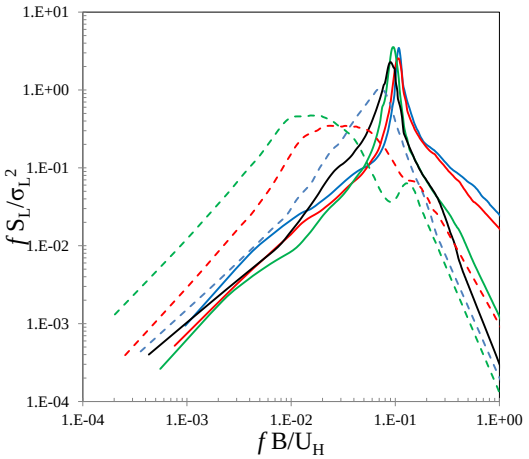

L/B=0.67，—：L/B=1，---：L/B=1.5，---：L/B=3，---：L/B=5

Acrosswind ESWL model

The background part of ESWL, $F_{L,B}(z)$ is given by:

$$F_{L,B}(z) = \rho U_H^2 C_L B \tag{1}$$

In which, C_L is the overturning moment based spatial averaged fluctuation lift force coefficient, and given by:

$$C_L = \sigma_L \Big/ \tfrac{1}{2}\rho U_H^2 BH^2 \tag{2}$$

σ_L is the RMS of wind tunnel measured base moment. The resonant part of the equivalent static load is assumed to have same distribution as the inertia force. Assuming the building mass is uniformly distributed along building height and the fundamental mode shape assumed to have the form of $\varphi(z)=(z/H)^{\beta}$. The resonant part of ESWL, $F_{L,R}(z)$ is given by:

$$F_{L,R}(z) = (2\beta+1)\frac{1}{H}\left(\frac{z}{H}\right)^{\beta}\left[\frac{\pi f_0 S_L(f_0)}{4\xi}\right]^{1/2} \tag{3}$$

Empirical formulae for lift coefficient and force spectra

The lift coefficient used in this article, C_L, is an overturning moment based spatial averaged force coefficient. In other words, the base moment calculated by adopting $F_{L,B}(z)$ along building height would be same as the wind tunnel results. Generally speaking, lift coefficient is primarily a function of building side ratio, *L/B*. Building aspect ratio and terrain condition cast secondary effects. This paper proposes the following form for C_L:

$$C_L = \ell_1\left(\frac{L}{B}\right)^3 + \ell_2\left(\frac{L}{B}\right)^2 + \ell_3\left(\frac{L}{B}\right) + \ell_4\left(\frac{L}{B}\right)^{\ell_5}\left(\frac{H}{\sqrt{BL}}\right)^{\ell_6} \tag{4}$$

The values for ℓ_i in three terrain categories are listed in Table 1.

	ℓ_1	ℓ_2	ℓ_3	ℓ_4	ℓ_5	ℓ_6
BL-A	0.0047	-0.03	0.19	-0.006	1.7	0.67
BL-B	0.0106	-0.09	0.25	-0.04	0.13	-0.01
BL-C	0.0144	-0.13	0.39	-0.018	0.53	-0.13

Table 1. Coefficients for C_L in equation (4)

The acrosswind forces acting on the buildings are the combined results of vortex shedding, lateral turbulence and end effects. For rectangular shaped tall buildings, the acrosswind force spectra are complex function of several variables: *L/B*, $H/\sqrt{BL}$, wind speed gradient and turbulence intensity. Although it is unrealistic to derive an analytical model that fully reflects the nature of acrosswind phenomenon. This paper intents to develop an empirical model with parameters containing clear physical meanings. Vickery & Clark (1972) based on the assumption that, in turbulent flow, vortex shedding frequency has nature of Gaussian process and proposed the famous lift force spectrum for circular cylinder:

$$\frac{fS_L(f)}{\sigma_L^2} = \frac{(f/f_s)}{\sqrt{\pi}B_e}\exp\left[-\left(\frac{1-(f/f_s)}{B_e}\right)^2\right] \tag{5}$$

In which, *fs* is vortex shedding frequency and B_e is spectral bandwidth. In later years, similar spectral formulations had been used for rectangular buildings with little success. That is because lateral turbulence and reattach phenomenon play important role in the acrosswind loads of rectangular shaped tall buildings and cannot be ignored as in the case of circular cylinder. Based on the aforementioned observations, this article proposes the following empirical model for the generalized acrosswind force spectra of rectangular shaped tall buildings:

$$\tilde{S}_L(f) = \frac{fS_L(f)}{\sigma_L'^2} = \sum_{i=1}^{2} S_{Li}(f)$$
$$L/B \le 2,\ i=1; \qquad L/B > 2,\ i=1,2 \tag{6}$$

In which, σ_L' is the RMS of the generalized lift force spectrum. The first term, $S_{L1}(f)$, represents contribution from vortex shedding process. The second term, $S_{L2}(f)$, represents contribution from the reattachment phenomenon. It is noted that the effect of lateral turbulence is not considered in this model. Initial study indicates that lateral turbulence has negligible effects on the low frequency components of lift spectrum. The resonant component of tall buildings usually acquires spectral estimates in the frequencies higher than the vortex shedding frequency. Therefore, the lateral turbulence was excluded to keep the empirical model from too complicated. $S_{L1}(f)$ and $S_{L2}(f)$ have the general form of:

$$S_{Li}(f) = A_i \exp\left[-\left|\frac{1-f/f_{si}}{Be_i}\right|^{\gamma_i}\right],\ i=1,\ 2 \tag{7}$$

In Which, A_1 and A_2 are magnitude of spectral estimates at the centre frequencies of vortex shedding and reattachment, respectively. Both A_1 and A_2 are functions of building side ratio, aspect ratio and terrain condition. Coefficients C_1 to C_4 in Eq. (8) and listed in Table 2 have different values for three terrain categories.

$$A_1 = C_1 * (\frac{L}{B})^{C_2} * (\frac{H}{\sqrt{BL}})^{C_3}$$
$$A_2 = C_4 * (\frac{L}{B})^{0.11} * (\frac{H}{\sqrt{BL}})^{0.2} \quad (8)$$

f_{s1} and f_{s2} are center frequencies of vortex shedding and reattachment phenomenon, respectively. Vortex shedding frequency, f_{s1}, is mainly a function of building side ratio, L/B, only. Center frequencies for reattachment, which is valid only for $L/B>2$, is a function of aspect ratio as shown in Eq. (9).

$$f_{s1} = -0.03 * (\frac{L}{B})^{0.7} + 0.12$$
$$f_{s2} = -0.01 * (\frac{H}{\sqrt{BL}})^{0.7} + 0.17 \quad (9)$$

Be_1 and Be_2 are spectral bandwidth near vortex shedding frequency, f_{s1}, and reattachment center frequency, f_{s2}. At each terrain category, Be_1 is function of side ratio, L/B, and longitudinal turbulent intensity, I_u, at two-third of building height. Be_2 is a function of side ratio only. Experimental data reveals that the spectral bandwidth of vortex shedding, Be_1, varies significantly between short rectangular shape, $L/B<1$, and long rectangular shape, $L/B>1$. Therefore, coefficient C_5 has two sets of values for different side ratio as listed in table 3.

$$Be_1 = C_5 \left(\frac{L}{B}\right)^{C_6} (I_u)^{C_7}$$
$$Be_2 = C_8 \left(\frac{L}{B}\right)^{0.01} (I_u)^{-0.03} \quad (10)$$

γ_i represents the rate of energy decay as frequency away from the spectral peaks, i.e., f_{s1} and f_{s2}. Unlike a constant value, $\gamma=2$ for circular cylinder, values of γ_i decrease in a rather complex manner. When contribution from vortex shedding decay rapidly as frequency distanced from the vortex shedding/reattachment frequencies, f_{si}, the contributions from lateral turbulence and end effects would compensate the energy loss and slow down the rate of energy decay. Let

$$f_i^* = \frac{|1 - f / f_{si}|}{Be_i} \quad , \quad i = 1, 2$$
$$f_i^* \le \tilde{f}, \quad \gamma_i = 2$$
$$f_i^* > \tilde{f} \quad \gamma_i = 2 - C_9 * (\frac{L}{B})^{C_{10}} (\frac{H}{\sqrt{BL}})^{C_{11}} \left(\frac{\tilde{f}}{f_i^*} - 1\right)^2 \quad (11)$$

In which, $\tilde{f} = 0.4$ for terrain *A* and *B*, $\tilde{f} = 0.6$ for terrain *C*.

Terrain	C_1	C_2	C_3	C_4	C_6
A	0.18	-1.0	0.6	0.015	0.4
B	0.2	-1.0	0.83	0.045	0.68
C	0.25	-0.97	0.83	0.15	0.72
Terrain	C_7	C_8	C_9	C_{10}	C_{11}
A	1.71	0.59	1.54	-0.08	-0.03
B	1.57	0.45	1.54	-0.08	-0.03
C	0.82	0.38	1.65	-0.07	-0.06

Table 2. Empirical coefficients in spectral models

Terrain	$0.2 \leqq L/B < 1.0$	$1.0 \leqq L/B \leqq 5.0$
A	6.28	11
B	6.86	9
C	2.1	2.4

Table 3. Values for C_5 in equation (10)

Accuracy of empirical models and parameters

Shown in Figure 3 are comparison of lift coefficient between proposed model, Eq. (4), and wind tunnel measurements. Figure 3 shows that, except small number cases of under-estimation in flow fields *BL-B* and *BL-C*, Eq. (4) predicts satisfactory values for C_L within 10% error marked by the two dash lines. Examine center frequency of vortex shedding, f_{s1}, from wind tunnel data reveals that vortex shedding frequency, f_{s1}, is primarily a function of side ratio, L/B, only. The empirical formula for f_{s1} performs quite well. Except over-estimated for some cases in flow field *BL-C*, the values given by empirical formula agree well with wind tunnel data.

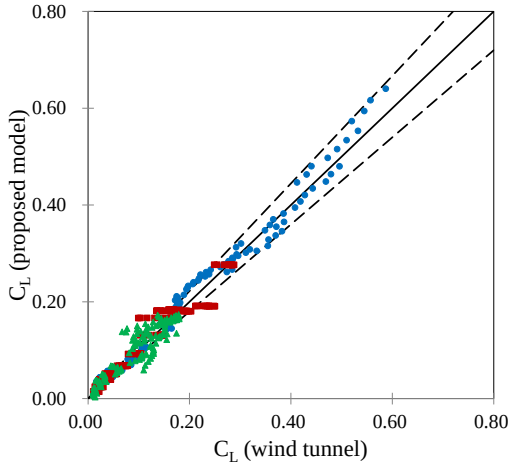

Figure 3. Comparison of acrosswind force coefficient C_L in equation (4). ●: BL-A，■: BL-B，▲: BL-C.

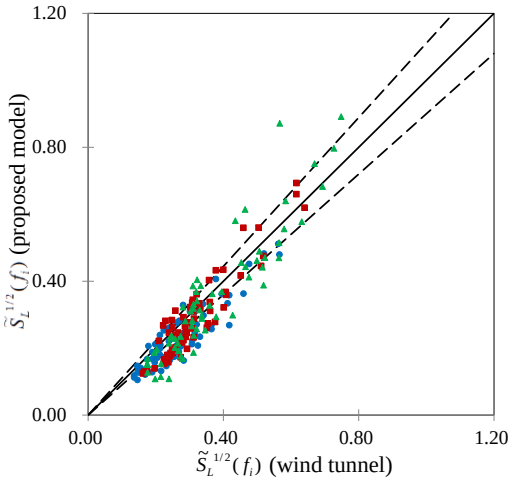

Figure 4. Comparison of reduced spectral estimates, $\tilde{S}_L(f_i)$. ●: BL-A，■: BL-B，▲: BL-C.

The square root of spectral estimates at a building's natural frequency is proportional to the resonant part of design wind loads. Hence, the square root of spectral estimates at all prototype building's natural frequencies were used for comparison between proposed model and wind tunnel data, as shown in Figure 4. Figure

4 indicates that the proposed acrosswind force spectra model performs better in flow *BL-A* and *BL-B*. In flow field *BL-C*, especially for buildings with side ratio *L/B*=0.67, the empirical model is over-conservative.

Case study

A group of prototype tall buildings were chosen to study the design wind loads. Assuming all buildings have the identical cross-sectional area, (*BL*)=900 m^2, and same story height, *h*=3.6 m. For example, a building with side ratio L/B=1/3 and aspect ratio $H/\sqrt{BL}$=6 would be a 50-story building with 52m in breadth, 17.3m in depth and 180m in height. The natural periods were assuming to be one-tenth of the story number in seconds. Damping ratio to be 0.01 for all buildings. Total of 78 prototype tall buildings were used, in each three terrain categories. The acrosswind design wind loads were estimated and henceforward to calculate the overturning moments.

The comparison of buildings overturning moment calculated from proposed acrosswind ESWL model and the value based on wind tunnel data is plotted in Figure 5. The proposed ESWL model performed quite well; for most cases, the results are within 10% error bound.

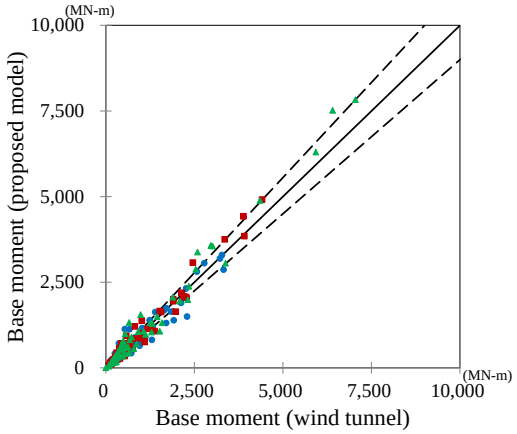

Figure 5. Comparisons of prototype buildings' base moments. ●: BL-A，■: BL-B，▲: BL-C.

Conclusions

In this article, an acrosswind equivalent static wind load model for rectangular shaped tall buildings were proposed based on wind tunnel data. In the proposed acrosswind force spectral model, specific physical meanings are given to the key parameters. In such a way, not only the empirical model is more in line with current understanding on building acrosswind loads, this model can be improved by others with support of additional data. The lift coefficients and spectral estimates produced by the proposed model were compared with wind tunnel measurements with satisfactory results. On the final stage, a large number of prototype tall buildings were used to study the model performance in term of building overturning moment. For most cases, the base moment yielded by proposed ESWL model are within 10% error bound.

References

[1] ASCE7-16, 2016. Minimum design loads for buildings and other structures.

[2] AIJ-2004. Architectural Institute of Japan. Recommendations for Loads on Buildings.

[3] AS/NZ1170.2:2011. Australian/New Zealand Standard on Wind Actions.

[4] CHENG C M, WANG J, CHANG C H. 2008. E-wind: An integrated engineering solution package for wind sensitive buildings and structures. Proceedings of the Third International Symposium: Wind Effects on Buildings and Urban Environment. Tokyo, Japan. 127-136.

[5] DAVENPORT A G. 1968. The dependence of wind load upon meteorological parameters. Proceedings of the international research seminar on wind effects on buildings and structures. Toronto, Canada. 19-82.

[6] GU M, QUAN Y. 2004. Across-wind loads of typical tall buildings[J]. Journal of Wind Engineering and Industrial Aerodynamics. 92(13): 1147-1165.

[7] KAREEM A. 1990. Measurements of pressure and force fields on building models in simulated atmospheric flows[J]. Journal of Wind Engineering and Industrial Aerodynamics. 36(1990): 589–599.

[8] KOPP G A, Y. CHEN Y. 2006. Database-Assisted Design of Low-Rise Buildings: Aerodynamic Considerations for a Practical Interpolation Scheme[J]. ASCE Journal of Structural Engineering. 132(2006): 909-917.

[9] KWON D, KIJEWSKI-CORREA T, KAREEM A. 2008. E-analysis of high-rise buildings subjected to wind loads[J]. ASCE Journal of Structural Engineering. 133(7):1139-1153.

[10] LIANG S, LIU S, LI Q S, ZHANG L, GU M. 2002. Mathematical model of acrosswind dynamic loads on rectangular tall buildings[J]. Journal of Wind Engineering and Industrial Aerodynamics. (90):1757–1770.

[11] QUAN Y, TAMURA Y, MATSUI M, CAO S Y, YOSHIDA A, 2007, TPU aerodynamic database of low-rise buildings, Procedings of 12th International Conference on Wind Engineering. Cairns, Australia. (2):1615-1622.

[12] TANG Y, GU M, QUAN Y. 2010. Fluctuating force of across-wind acting on rectangular super-tall buildinds, Part II: Mathematical model[J]. Journal of Vibration and Shock. 29(6). (in Chinese)

[13] VICKERY B J, CLARK A W. 1972. Lift or crosswind response of slender stack[J]. ASCE Journal of Structural Engineering. 98(1).

[14] ZHOU Y, KAREEM A. 2001. Gust loading factor: new model[J]. ASCE Journal of Structural Engineering. 127(2): 168-175.

[15] ZHOU Y, KIJEWSKI T, KAREEM A. 2003. Aerodynamic loads on tall buildings: interactive database[J]. ASCE Journal of Structural Engineering. 129(3): 394-404.